



INSTITUT DE FRANCE
Académie des sciences

Comptes Rendus

Physique

Michael Le Bars, Louis-Alexandre Coustou, Benjamin Favier, Pierre Léard, Daniel Lecoanet and Patrice Le Gal

Fluid dynamics of a mixed convective/stably stratified system—A review of some recent works

Volume 21, issue 2 (2020), p. 151-164

Published online: 3 November 2020

Issue date: 3 November 2020

<https://doi.org/10.5802/crphys.17>

Part of Special Issue: Prizes of the French Academy of Sciences 2019

 This article is licensed under the
CREATIVE COMMONS ATTRIBUTION 4.0 INTERNATIONAL LICENSE.
<http://creativecommons.org/licenses/by/4.0/>



Les Comptes Rendus. Physique sont membres du
Centre Mersenne pour l'édition scientifique ouverte
www.centre-mersenne.org
e-ISSN : 1878-1535



Prizes of the French Academy of Sciences 2019 / *Prix 2019 de l'Académie des sciences*

Fluid dynamics of a mixed convective/stably stratified system—A review of some recent works

Dynamique des fluides d'un système mixte convectif / stablement stratifié — Une revue de quelques travaux récents

Michael Le Bars^{*, a}, Louis-Alexandre Coustou^a, Benjamin Favier^a,
Pierre Léard^a, Daniel Lecoanet^b and Patrice Le Gal^a

^a CNRS, Aix Marseille Univ, Centrale Marseille, IRPHE, Marseille, France

^b Princeton Center for Theoretical Science and Department of Astrophysical Sciences,
Princeton, New Jersey 08544, USA

E-mails: lebars@irphe.univ-mrs.fr (M. Le Bars), lacoustou@gmail.com
(L.-A. Coustou), favier.benjamin@gmail.com (B. Favier), pierre.leard@gmail.com
(P. Léard), dlecoanet@gmail.com (D. Lecoanet), legal@irphe.univ-mrs.fr (P. Le Gal)

Abstract. Numerous fluid systems organise into a turbulent layer adjacent to a stably stratified one, for instance, planetary atmospheres and stellar interiors. Capturing the coupled dynamics of such systems and understanding the exchanges of energy and momentum at the interface between the two layers are challenging, because of the large range of involved time- and length-scales: indeed, the rapid small-scale turbulence excites waves at intermediate scale, which propagate and interact non-linearly to generate large-scale circulations, whose most famous example is the quasi-biennial oscillation of the Earth's atmosphere. We review here some recent progress on the wave characterisation and on the non-linear mean flow generation, based on the combined experimental and numerical study of a model laboratory system. Applications in climate and stellar modelling are also briefly discussed.

Résumé. De nombreux systèmes fluides s'organisent en une couche turbulente adjacente à une couche stratifiée stable, comme par exemple les atmosphères planétaires et les intérieurs stellaires. La compréhension des échanges d'énergie et de quantité de mouvement à l'interface entre ces deux couches, et l'appréhension de leur dynamique couplée sont difficiles, en raison de la grande gamme d'échelles de temps et de longueur impliquées : en effet, la turbulence rapide à petite échelle excite des ondes à moyenne échelle, qui se propagent et interagissent non linéairement pour générer des circulations à grande échelle, dont le plus célèbre exemple est l'oscillation quasibiennale de l'atmosphère terrestre. Dans cet article, nous passons en revue

* Corresponding author.

quelques progrès récents sur la caractérisation des ondes et sur la génération non-linéaire d'un écoulement moyen, obtenus par l'étude combinée, expérimentale et numérique, d'une configuration modèle au laboratoire. Les conséquences possibles de nos résultats pour la modélisation climatique et stellaire sont aussi brièvement discutées.

Keywords. Internal gravity waves, Convection, Wave—mean flow interactions, Quasi-biennial oscillation (QBO), Atmospheric and stellar dynamics.

Mots-clés. Ondes internes de gravité, Convection, Interactions ondes — écoulement moyen, Oscillation quasi-biennale, Dynamique atmosphérique et stellaire.

2020 Mathematics Subject Classification. 76-XX.

1. Introduction

Numerous natural systems exhibit a specific organisation with a turbulent convective layer adjacent to a stably stratified one: examples include planetary atmospheres with their troposphere/stratosphere, and stellar interiors with their convective/radiative zones. The dynamics of such coupled, two-layer systems are quite complex and scatter over large ranges of time-scales and length-scales. Indeed, motions in the convective layer excite internal gravity waves (IGWs) which propagate from the interface into the stratified region, sustained by gravity and the progressive decrease of the ambient density profile (for a full description of IGWs and their properties, see [1]). IGWs carry momentum and energy, and are thus to be accounted for closing the energy budget of such coupled systems, in order to make e.g. relevant mid- and long-term climate prediction. Waves are also of direct interest in e.g. asteroseismology to probe otherwise inaccessible stellar interiors [2]. Besides, waves can non-linearly generate large scale horizontal flows with global, long-term, dynamical consequences. Such a mechanism has for instance been invoked to explain the apparent misalignment of some exoplanets around hot stars [3]. But its most striking evidence is the quasi-biennial oscillation (QBO) of the Earth's atmosphere at altitudes ranging from about 16 to 50 km, corresponding to a nearly periodic reversal of the equatorial stratospheric winds between easterlies and westerlies with a mean period of 28 to 29 months [4]. Similar oscillations have also been reported in Jupiter's and Saturn's atmospheres [5, 6].

The QBO is classically explained by the specific “anti-diffusive” nature of IGWs (e.g. [7]): IGWs are more prone to lose momentum when they propagate in the same direction as the ambient flow, which in turn is reinforced by the deposition of wave momentum. The mechanism for energy dissipation and wave damping can be due to different phenomena such as radiation, wave breaking and interaction with critical levels in atmospheres and stars, viscous dissipation in experiments... In all cases, as illustrated in Figure 1 (left), starting from e.g. an eastward wind (horizontal mean flow \bar{u}) plus two IGWs emitted at the interface with the same frequency and amplitude but with opposite directions, the eastward-propagating wave rapidly deposits its energy and locally increases the ambient wind, while the westward-propagating wave rises higher up and finally damps while generating a westward wind at larger altitude. This appealing mechanism was theorised in [7–9] in a one-dimensional (1D) model solving only for the mean flow equation in the linearly stratified domain: there, the time derivative of the mean flow equals its viscous dissipation plus a source term coming from the momentum flux from damped fluctuations (i.e. the vertical gradient of their associated Reynolds stress, corresponding to the horizontal average of the product of the horizontal and vertical velocity fluctuations); it was evaluated analytically by

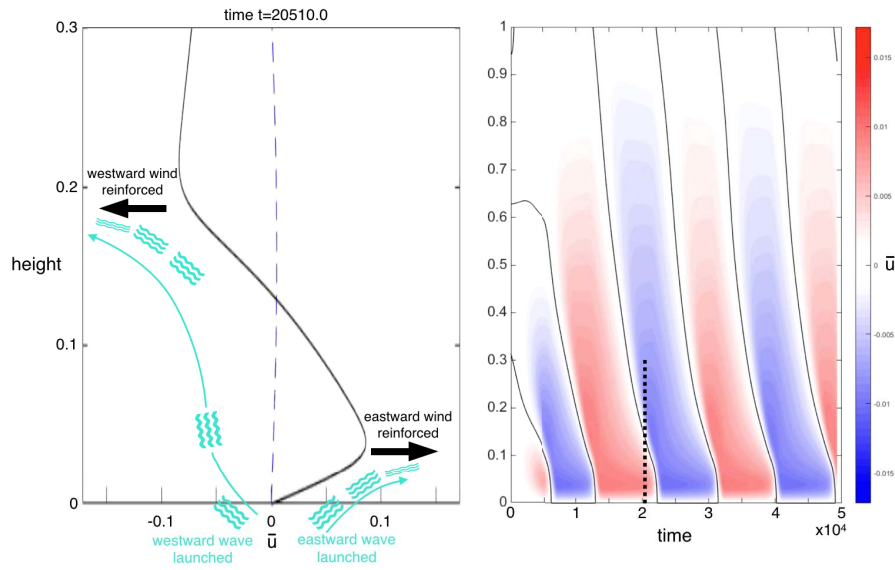


Figure 1. Sketch of the classical QBO model of Lindzen–Holton–Plumb [7–9] (left) and time evolution of the horizontal mean flow \bar{u} as a function of depth computed from the associated 1D model, solving for the mean flow in the presence of a monochromatic, linear wave source in the WKB limit (right). On the left, the dashed line shows the initial mean flow profile and the solid line the profile at $t = 20510$, shown as a vertical dotted lined on the right. Time is adimensionalised by the buoyancy frequency N and lengths by the domain height H .

considering the weakly damped, Doppler shifted, linear internal gravity waves in the WKB limit (i.e. assuming scale separation between the waves and the mean flow) (see details in e.g. [10]). An example of obtained QBO is shown in Figure 1 (right). The monochromatic QBO mechanism was also demonstrated experimentally in the famous study by Plumb and McEwan [11], recently extended by Semin *et al.* [12]: they used oscillating membranes at the boundary of a linearly-stratified salty-water layer in order to force a standing wave pattern in a cylindrical shell container, mimicking the equatorial stratospheric band. However, in this classical model of the QBO and in its experimental realisation, the wave forcing remains steady and monochromatic, as opposed to the atmospheric configuration where it is due to turbulent tropospheric motions [4]. Besides, the excitation is driven by forced interface displacements and only the stratified layer is modelled, neglecting any coupling with the turbulent source. In Global Climate Models (GCMs) capable of spontaneously exhibiting a QBO, part of the waves responsible for its generation, including non-orographic IGWs excited by moist convection [13], are not resolved: they have to be parameterized, and the chosen parameterization scheme significantly affects the obtained results [14, 15]. It thus remains a challenge to observe and understand if/how/when a large-scale, reversing flow spontaneously emerges from a wide range of naturally excited IGWs, in a self-organising coupled two-layer system. And even before doing so, deciphering the mechanism of wave excitation in such a coupled convective/stably stratified system, as well as predicting the spectral characteristics of the associated wave field, are still debated. These are the tasks we have started to tackle over the last few years combining experiments and numerical simulations. This paper presents a rapid review of our recent contributions [16–21] and of some of the remaining open questions.

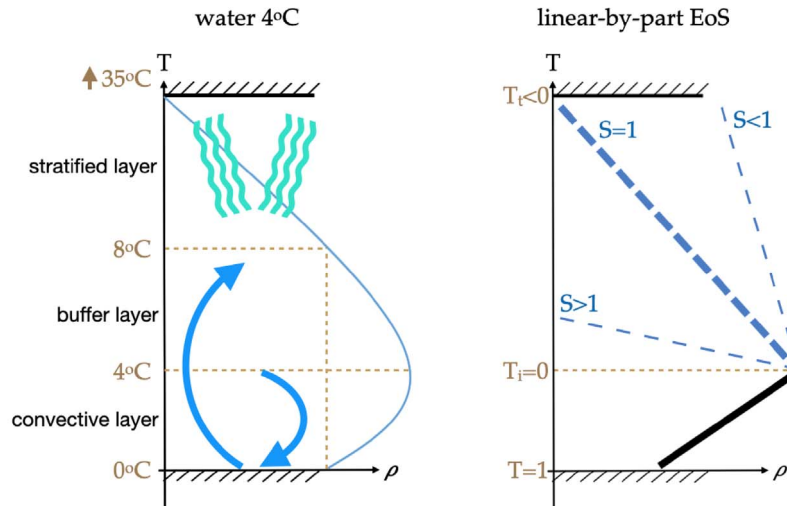


Figure 2. Density variation as a function of temperature for water around 4 °C (left) and for the generalised equation of state used in our numerical simulations (right).

2. Experimental and numerical investigation tools

2.1. A self-consistent two-layer system in the laboratory: convection in water around 4 °C

Previous studies of wave excitation by convection have used either a forced plume [22] or a transient Rayleigh–Bénard system, starting from a thermally stratified configuration and suddenly reversing the buoyancy profile from a boundary [23, 24]. But as first realized by Townsend [25], a self-organising, stationary, two-layer convective/stably stratified system can be relatively readily obtained in the laboratory using water, thanks to its specific property of having its maximum density at 4 °C with a nearly parabolic equation of state around it: as sketched in Figure 2 (left), in a simple reverse Rayleigh–Bénard configuration with cooling from below at 0 °C and heating from above at e.g. 35 °C, a two-layer system spontaneously emerges, with a turbulent convective layer below a stably-stratified one. Cold buoyant plumes rise from the bottom plate at 0 °C, cross the 4 °C isotherm, and theoretically equilibrate around the 8 °C isotherm, when neglecting diffusive effects; reciprocally, dense plumes at 4 °C detach from the maximum density interface and sink into the cooler, convective layer. IGWs propagate in the stably stratified layer above 8 °C. Note that because of the dissymetry between rising and sinking convective structures, the region between 4 °C and 8 °C is very specific: it is called the buffer layer [26].

Figure 3 shows our experimental realisation of this system [21], following an earlier, less evolved version of the set-up [16]. The tank is made of 2 cm thick acrylic sides, a temperature controlled bottom copper plate, and a transparent, temperature controlled, electric heater as a top boundary. Inner dimensions are $32 \times 32 \text{ cm}^2$ in horizontal and $H = 20 \text{ cm}$ in height. A cylinder of outer diameter 29 cm and thickness 0.4 cm might be centred inside this tank to obtain an axisymmetric geometry prone to the development of large-scale horizontal flows, as shown by the historical work of Plumb and McEwan [11]. Velocity measurements are performed in a vertical central plane using Particle Imaging Velocimetry (PIV), to characterize both convective motions and propagating IGWs (Figure 3 bottom left). Additionally, wave dynamics and the possible presence of large-scale horizontal flows are assessed by performing horizontal PIV (Figure 3 bottom right) and scanning over the whole depth of the tank. Further details on the experimental set-up can be found in [21].

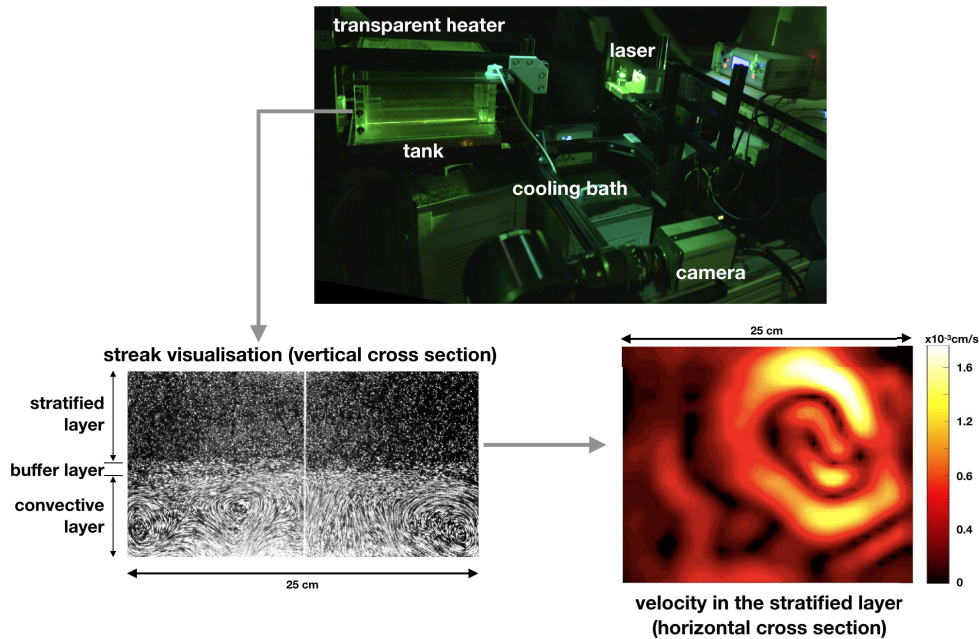


Figure 3. Picture of the experimental set-up (top) and illustration of velocity measurements in a vertical plane (bottom left) and in an horizontal plane (bottom right). The vertical cross-section shows a streak pattern obtained by superimposing 15 images (i.e. duration of 7.5 s) from the PIV acquisition movie. The horizontal cross-section shows an instantaneous PIV field in the stratified domain, at a distance ~ 1 cm above the interface with the convective zone.

This experimental system is fully characterised by 3 dimensionless parameters, defined as

- the Prandtl number $Pr = \nu/\kappa$, equal to the ratio of kinematic viscosity ν to thermal diffusivity κ averaged over the whole domain,
- the Rayleigh number Ra based on the convection-driving density difference $\Delta\rho = \rho(4^\circ\text{C}) - \rho(0^\circ\text{C})$, $Ra = g\Delta\rho H^3/\rho_0\kappa\nu$, where g is the gravity and ρ_0 the mean density,
- the top temperature anomaly relative to the “inversion” 4°C temperature, non-dimensionalised by the convection-driving temperature difference (0°C to 4°C here), named T_t .

We also define the mean buoyancy frequency N from the total density contrast over the stratified layer depth. In our experiment, $Pr = 7$, $Ra = 7 \times 10^6$, $T_t = -7.75$, and $N = 0.135$ Hz. As illustrated in Figure 3, the flow in the convective region is chaotic, with turbulent plumes advected by large-scale circulation and typical velocities around 1 mm/s. The buffer layer is clearly apparent, subject to a strong horizontal shear discussed in details in [21]. The stratified domain sustains IGWs with typical velocities around $10 \mu\text{m/s}$: they appear in the horizontal cross-section as concentric rings, similar to waves propagating from an impact point at the surface of a lake.

2.2. Generalisation in direct numerical simulations

While convection in water around 4°C allows a nice experimental realisation of a self-consistent, two-layer configuration, it is also intrinsically limited in terms of parameter space exploration. Indeed, considering a fixed total domain size, we have two adjusting parameters: the top and bot-

tom temperatures. We aim at maximising the Rayleigh number to reach a chaotic state: we thus use the maximum possible driving temperature contrast, hence a bottom temperature of 0°C . Adjusting the top temperature anomaly allows changing the relative depth of the two layers. However, at steady-state, heat flux conservation between the convective and the stratified domains intrinsically fixes the value of the buoyancy frequency: indeed, according to the Howard's historical scaling law [27], the convective heat flux does not depend on the convective layer depth, but only on its driving temperature difference, which is here fixed at 4°C ; this fixes the temperature gradient in the diffusive, stratified layer, which determines the buoyancy frequency. Besides, we aim for a deep enough stratified layer to allow for wave propagation, and lateral heat losses render the system highly non-linear (see e.g. discussion in [17]): this significantly limits any change in the temperature anomaly. Finally, using water also fixes the value of the Prandtl number to 7, which is limiting since as we show in the following, Pr has a tremendous influence on the long-term dynamics. Hence, to further explore the dynamics of our self-organising two-layer system, we have also used numerical simulations, expanding upon the experimental model.

We have first solved the non-Oberbeck Boussinesq Navier–Stokes and temperature equations using the approximate parabolic equation of state for water, hence closely reproducing the experiments. To do so, we have used either the open spectral solver Dedalus [28] in two dimension (2D), with periodic horizontal boundary conditions [17], or the open spectral element solver NEK5000 [29] in three dimension (3D), with perfectly insulating, rigid vertical boundaries [21]. As will be detailed in the following, this has allowed us to investigate the mechanism of wave excitation [17], to assess the experimental uncertainties issued from e.g. non-perfect thermal boundary conditions, and to explore the influence of the Prandtl number on the dynamics [21].

Then, to provide a more systematic exploration of a larger parameter space, we have also considered an equation of state with a constant thermal expansion coefficient in each layer, but changing sign and value around a chosen inversion temperature (Figure 2 right). Non-Oberbeck Boussinesq Navier–Stokes and temperature equations are then solved using the open spectral solver Dedalus [28] with periodic boundary conditions in the horizontal direction, both in 2D [18, 19] and in 3D (see [20] and Figure 4 left). The ratio S of the thermal expansion coefficients in the stratified vs. convective layers determines the stiffness of the interface, and reveals three different regimes (see Figure 4 right and [18]): a whole-layer convective regime at small stiffness, where the interface is destroyed by rising plumes; a two-layer regime at large stiffness, where the interface remains flat but gravity internal modes are excited by Reynolds stress fluctuations from the convective layer; and an intermediate regime in between, with a deformable interface and propagating IGWs, actually corresponding to the experimental, water configuration. In the following, we will focus on this last case only.

3. Wave properties

3.1. Mechanism for wave excitation

A good knowledge of the physical mechanism for wave excitation is fundamental for correct IGW parameterization in climate models and valid interpretation of asteroseismology observations (see e.g. [30]): as reviewed for instance in [22], it is thus the subject of a long-standing debate, with two main possible models sketched in Figure 5. In the mechanical oscillator model, convective updrafts rise up and deflect the interface with the stratified zone, hence locally initiating propagating IGWs. On the contrary, the deep forcing model assumes excitation all over the convective domain from the Reynolds stress associated with turbulent fluctuations: generated IGWs are first evanescent in the convective domain where no global stratification exists, and turn into propagating IGWs if/when they reach the interface and the stratified domain.

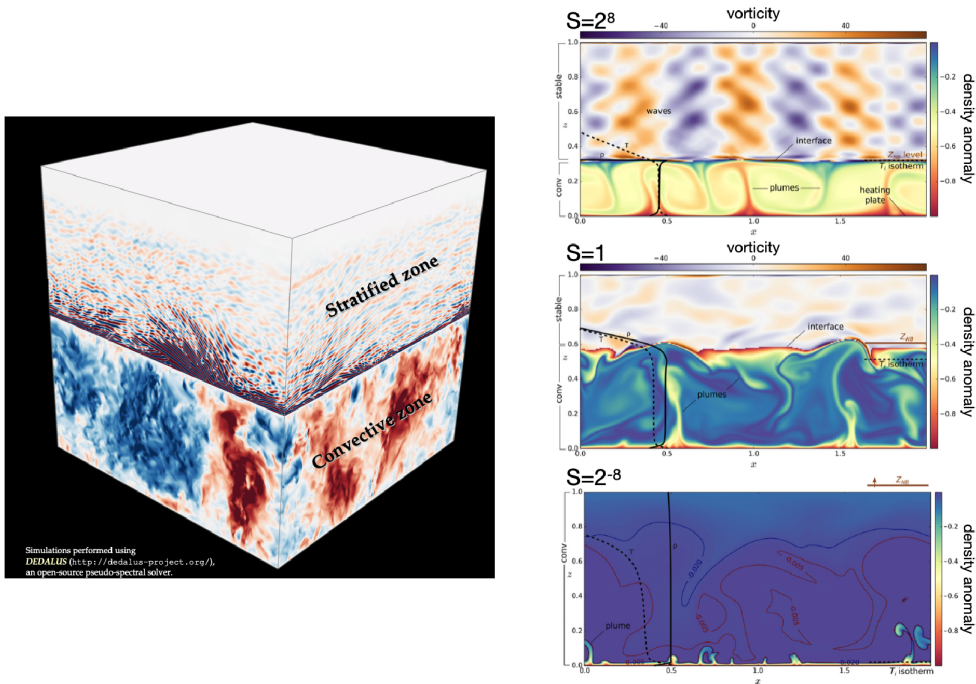


Figure 4. Snapshots from numerical simulations at thermal equilibrium using a piecewise linear equation of state. Left: vertical velocity in a 3D simulation for $Ra = 2 \times 10^8$, $Pr = 1$, $T_t = -52$ and $S = 400$, with red corresponding to upward motions and blue to downward motions. Note that the color scale is adjusted in each zone separately for better visualization. Right: 2D simulations for a given $Ra = 8 \times 10^7$, $Pr = 1$, $T_t = -20$, and 3 different stiffnesses S representative of the 3 different regimes of the system's dynamics, reproduced from [18]. Colors show the density anomaly in the convection zone below the neutral buoyancy height noted Z_{NB} , and the vorticity in the stratified zone above it (except for the smaller value of S where Z_{NB} is outside of the domain). We also show the mean temperature and mean density profiles as dashed and solid lines.

To quantitatively assess which model is the most relevant for our configuration, we use a 2D full simulation of the water experiment, together with 2 models of the simulation where we only solve for the linear wave equation in terms of vertical displacement, together with an adhoc source of excitation. The flexibility of the Dedalus solver [28] is especially suited for this type of approach. The first model of the simulation corresponds to the deep forcing, where we follow the approach of Lighthill [31], adapted to our configuration: we first compute from the full simulation the Reynolds stress all over the convective domain, and we then use it as the excitation term in the wave equation, with a buoyancy frequency equal to zero in the convective domain and to its horizontal and temporal average in the stratified domain. The second model of the simulation corresponds to the mechanical oscillator mechanism: we calculate from the full simulation the position of a chosen isotherm as a function of time. We then use these position fluctuations as the bottom boundary condition for the wave displacement in the model, solving wave propagation in the stratified domain above this isotherm only. We have considered 2 different isotherms encompassing the effective interface location: the 5°C which is very close to the density maximum, and the 8°C which corresponds to the maximum height of rising plumes at 0°C in the absence of dissipation (since the equation of state is parabolic with a maximum at 4°C).

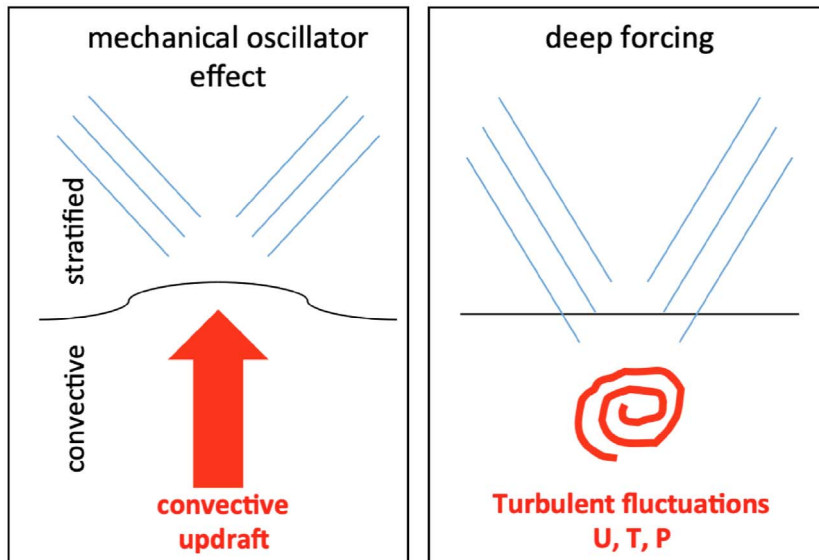


Figure 5. Sketch of the two possible mechanisms for IGW excitation from convection.

Comparison between the full simulation and the 2 models is shown in Figure 6, considering the power spectrum density of the vertical velocity as a function of depth in the stratified region. The deep forcing model agrees remarkably well with the full simulation, while the mechanical oscillator model exhibits high frequency IGWs with overestimated amplitude. The interface forcing considers plumes hammering on the interface, hence produces impulsive excitations that translate into high-frequency waves; it does not correctly account for the regularisation/smoothing of the complete flow, like e.g. the sweeping motions along the interface of the thermal uplifts advected by the large-scale convective motions shown in Figure 3. Comparing Figures 6(c) and (d), it is clear that the forcing by the 8 °C isotherm fluctuations does a much better job, as one would expect from the fact that by then, wave amplitudes are small and the dynamics is much more linear. Nevertheless, the high-frequency signature in the spectrum is still very apparent, contrary to both the full simulation and the bulk forcing model. In conclusion, and even if in visualizations we clearly see strong, but intermittent evidences of the mechanical oscillator in the form of wave clusters emerging from impinging rising plumes (see e.g. Figure 4(left)), the wave energy distribution is clearly dominated by the Reynolds stress coupling with the convective layer. It is thus better described by a deep forcing model, at least in the explored range of parameters.

3.2. Wave flux

Acknowledging that deep forcing by Reynolds stress is the predominant source of IGWs, it is possible to compute the full temporal and spatial spectrum of linear waves in the stratified region from an adhoc modelling of the turbulent region [32]. For instance, Lecoanet and Quataert [33] describe the flow in the convective region as a Kolmogorov turbulent cascade from an injection scale corresponding to the large-scale circulation. They then predict that for weakly damped waves, the energy flux spectrum scales like $k_{\perp}^4 f^{-13/2}$, where k_{\perp} and f are the wave horizontal wavenumber and frequency, respectively; the total wave flux decreases as a power law of the distance from the interface, with an exponent $-13/8$. Despite the simplicity of the underlying mechanistic model, this analytical prediction shows remarkable agreement with our

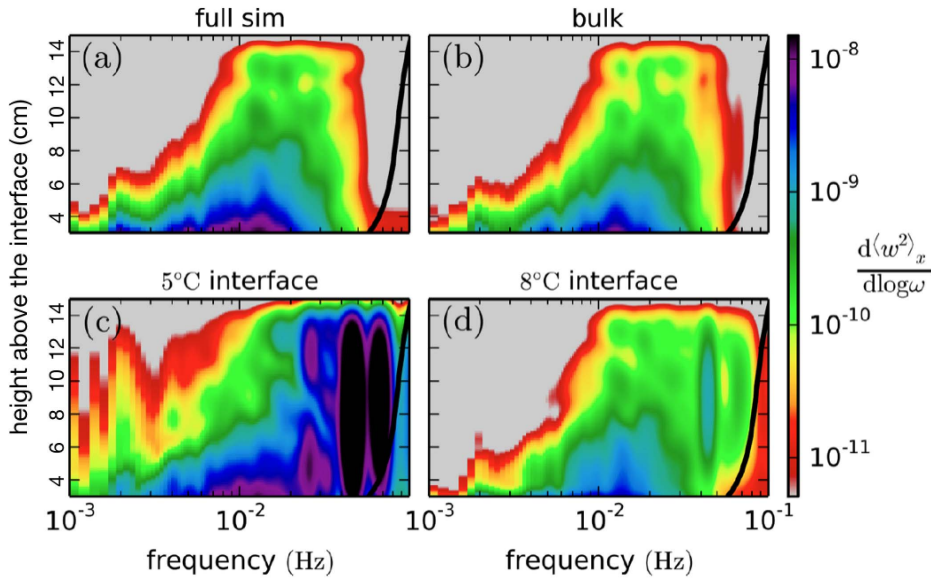


Figure 6. Spectrograms of the vertical velocity squared in the full simulation of the 4 °C experiment (a), in the deep forcing model (b) and in the mechanical oscillator model using the 5 °C (c) and the 8 °C (d) isotherms. The black line shows the horizontally and temporally averaged buoyancy frequency profile. Reproduced from [17].

3D simulations, as shown in [20] and illustrated in Figure 7. These scalings can thus be used to assess possible wave signatures revealed by asteroseismology. For instance, Bowman *et al.* [34] recently reported low-frequency photometric variability in a large number of hot massive stars, which they interpret as the surface signature of IGWs excited by the deep convective core [35]. If it was so, the analysis of those waves would provide a unique probe inside the otherwise inaccessible depths of those mysterious objects. However, the observed spectral signature does not match with our validated model, and we rather interpret it as the trace of some subsurface convection [30]. This issue is currently debated [36].

4. Mean flow generation and reversals in the stratified layer

4.1. Influence of the Prandtl number

Beyond IGWs characterization, we have also assessed the generation of a mean flow in the stratified region of our 4 °C experiment by systematically measuring the azimuthal mean of the azimuthal velocity as a function of depth and time: results are shown in Figure 8 (left). While the experimental velocity field exhibits reversals on a typical time much longer than the wave periods (7.4–250 s typically), the observed signal cannot be related to a QBO process, because the phase propagation of reversals goes slightly upward, as opposed to the clear downward signature observed both in atmospheric data [4] and in the ideal, 1D, monochromatic QBO model (Figure 1 right). By reproducing our experiment using 3D numerical simulation, we have checked that this signal is not due to any improper boundary condition, like e.g. lateral heat losses which could have induced unwanted natural convection [21]. Actually, an estimate of the viscous propagation of a velocity perturbation from the interface shows a quantitative agreement with the experimental signal (see dotted lines in Figure 8 left): the stratified layer is viscously coupled to the interface

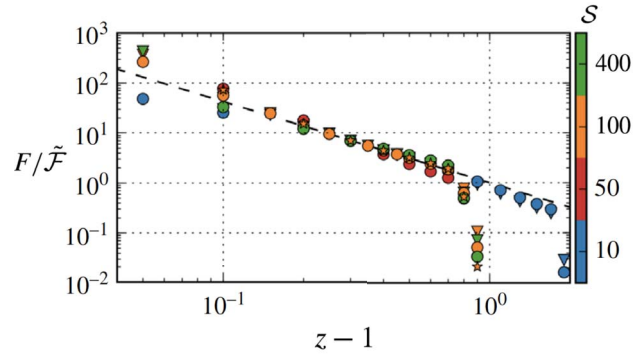


Figure 7. Total flux carried by IGWs in the stratified domain (normalised by its theoretical evaluation, see details in [20]), as a function of height above the interface located at $z = 1$. Triangles, circles and stars show results from our 3D simulations for $Ra = 4 \times 10^7, 2 \times 10^8, 10^9$, and the dashed line the theoretical scaling $(z - 1)^{-13/8}$. Color shows the stiffness S , $Pr = 1$ in all cases, and T_t is adjusted so as to conserve the same stratified layer depth. Deviations at small z are due to non-wave flows present around the interface region. Departure at large z comes from imposed boundary conditions in the simulations. Note that the simulations with $S = 10$ (i.e. blue color) were performed in a deeper computational domain, hence depart close to $z - 1 = 2$ instead of $z - 1 = 1$. Reproduced from [20].

region. In water, viscosity is indeed the dominant diffusive effect, as quantified by its Prandtl number $Pr = 7$. Reproducing the same two-layer configuration in a numerical simulation with $Pr = 0.1$ actually shows the vanishing of this viscous coupling as well as some tenuous signature of a QBO-like pattern [21].

The Prandtl number thus has a fundamental influence on the generated mean flow that we want to address systematically. However, such a study is extremely costly from a numerical point of view: it requires numerous and long computations with a highly performant solver, and remains barely feasible today in 3D. We have thus started this systematic study using our 2D Dedalus model with periodic boundary conditions and a piecewise linear equation of state [19]. Three illustrative results are shown in Figure 8 (right). At $Pr = 0.3$, a QBO is clearly observed; at $Pr = 1$, a QBO is obtained but is barely visible; and at $Pr = 3$, the QBO signature completely disappears and the mean flow has an upward phase suggestive of a viscous coupling with the convective region. The thresholds between these different regimes deserve a more detailed, dedicated study, and surely depend on the level of turbulence in the convective domain. Nevertheless, our first results here highlight that in numerical modelling of the long-term dynamics of an atmosphere ($Pr = 0.7$) or a star ($Pr = 10^{-5}$), the Prandtl number based on molecular viscosity and thermal diffusivity should not be fixed at 1 for numerical convenience, as commonly done.

4.2. Parameterisation of IGWs and the resulting QBO

Actually, computing the full dynamics of a two-layer system, including all the time- and length-scales of convection, of waves, and of their non-linear long-term interactions, remains limited to idealised or local configurations. In Global Climate Models (GCMs) for instance, physical variables are typically evaluated every ten minutes on a grid with 100 km resolution in the horizontal and a few hundred meters in the vertical (e.g. [37]); phenomena at smaller scales—like non-orographic IGWs—are not resolved but appear as parameterizations. Some GCMs are capable of

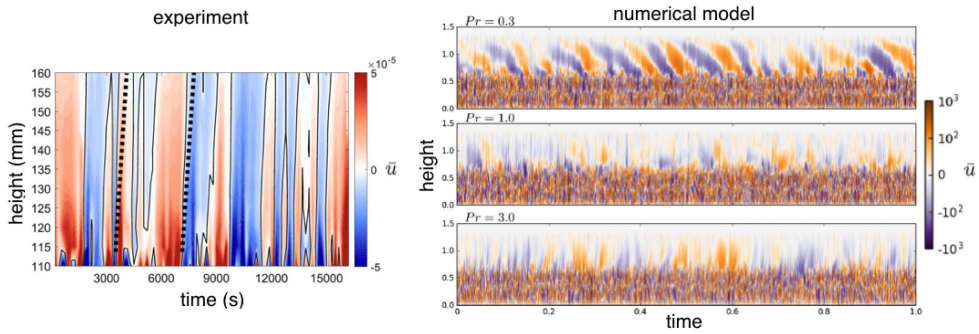


Figure 8. Evolution as a function of time and height of the azimuthal average of the azimuthal velocity in our 4 °C experiment where $Pr = 7$ (left), and of the horizontal average of the horizontal velocity for three 2D simulations with the piecewise linear equation of state considering $Pr = 0.3, 1, 3$ respectively (right). In numerical simulations, $T_t = -43$ and the other parameters are slightly adjusted to maintain the same depth and buoyancy frequency in the stratified region, i.e. $Ra = 8 \times 10^7, 5.6 \times 10^7, 4.4 \times 10^7$ and $S = 0.33, 0.14, 0.06$, respectively. Adapted from [21] and [19]. Note that the experimental results show the stratified domain only. The dotted lines show the typical viscous propagation of a perturbation from the interface.

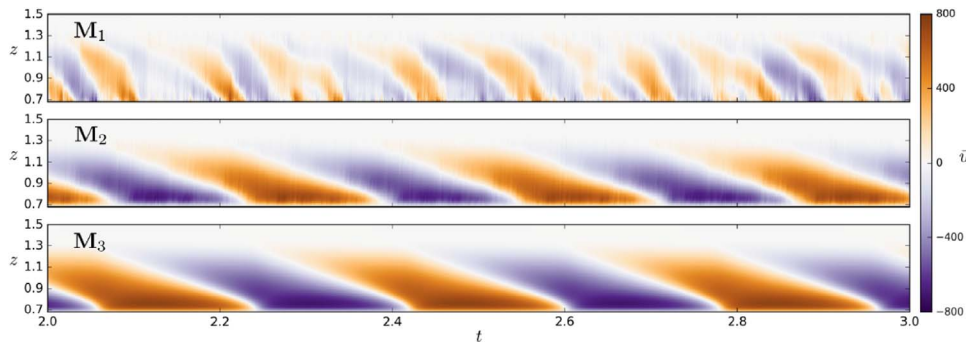


Figure 9. QBO-like flows produced in the stratified domain of a full 2D simulation of the coupled system (M1, same parameters as Figure 8 top right); in a 2D model of the stratified layer only, using as bottom boundary conditions the forcing extracted from the full simulation at the depth of neutral buoyancy (M2); and in a 1D Lindzen–Holton–Plumb-like model sustained with the energy spectrum measured at the interface of the full simulation (M3). Reproduced from [19].

producing realistic QBO (see e.g. [15] and references therein), whose signature provides a reliable test for proving the validity of the model [38]. However, different parameterization schemes lead to different predictions. In addition to very interesting, recent initiatives in assessing QBO modelling uncertainties by performing coordinated numerical benchmarks with GCMs [14, 15], our simplified model could offer a unique opportunity to assess the minimum necessary ingredients for a relevant treatment of IGWs and QBO.

Figure 9 (top) shows again the mean flow in the stratified layer from the full simulation at $Pr = 0.3$ introduced in Figure 8 (top right). The QBO signature is clearly visible. We then consider 2 models of the simulation. In M2 (Figure 9 middle), we solve the full Boussinesq Navier–Stokes

equations in the stratified layer only, using as bottom boundary conditions the forcing in velocity and temperature measured in the full simulation at the interface (i.e. depth of neutral buoyancy). Finally, bottom Figure (M3) shows results from a 1D Lindzen–Holton–Plumb-like model (i.e. solving only the mean flow equation with a forcing term computed from the weakly damped, Doppler shifted, linear internal gravity waves in the WKB limit), using as a forcing term the linear superimposition (with no cross-correlation) of a large range of wave contributions, each wave being excited with an amplitude given by the energy spectrum measured at the interface of the full simulation. Comparing M2 and M3 shows that the 1D Lindzen–Holton–Plumb-like model actually does a decent job in reasonably reproducing, at much lower numerical cost, the signal obtained from a given energy input at the interface, despite all underlying approximations (WKB, weakly damped IGWs, etc.). However, both models fail in predicting the relevant period and amplitude of flow reversals in the full simulation shown in M1, which reinforces the conclusion already raised in Section 3.1 on the source of IGWs: considering wave excited by interface fluctuations only is not sufficient for producing the relevant wave spectrum over the whole stratified domain, hence for correctly modelling their long-term non-linear effects. One must actually consider the whole Reynolds stress generated in the convective region. This is clearly not feasible for GCMs parameterization. But one should at least consider, beyond energy spectrum, higher order statistical description of the wave interface fluctuations, in order to better account for the properties of the convective turbulent source, including in particular intermittency and wave packet production: this is done for instance by [13].

5. Conclusion and open questions

In conclusion, by combining laboratory experiments and numerical simulations, we have successfully characterised the mechanism and characteristics of IGWs excitation in a self-organising two-layer convective/stably stratified system. Our model has also demonstrated that beyond the historical 1D, monochromatic model of Lindzen, Holton and Plumb [7–9], and in complement to GCMs where part of the relevant waves still have to be parameterized [15], slowly reversing mean flows may spontaneously emerge from a stochastic convective excitation, provided the Prandtl number is low enough. Various challenges now remain to be tackled. First from an experimental point of view, main challenges are: (i) to produce QBO-like reversals in a set-up with a stochastic excitation, and (ii) to explain why the only successful experimental QBO up-to-now has been obtained in salty water, i.e. with an equivalent Prandtl number of 700, which seems at odds with our previous conclusion. Then from a numerical point of view, main challenges are: (i) to obtain QBO-like reversals in 3D direct numerical simulations of the full coupled system, and (ii) to extend our results on wave excitation and propagation to more realistic configurations, including in particular compressibility and rotation effects [39], as well as a spherical geometry. Finally, beyond atmospheric and stellar applications, it would be of great interest to evaluate the consequences of waves in other natural two-layer systems, like e.g. the Earth's iron core, where the presence of a convective domain is the prevalent model for explaining the generation of the Earth's magnetic field, but where the presence of a stratified layer has recently been proposed [40]: as in stars and atmospheres, no doubt that excited waves and associated mean flow in this stratified layer would have a strong signature, here imprinted in the magnetic field [41].

Acknowledgements

The authors are supported by the European Research Council under the European Union's Horizon 2020 research and innovation program through Grant No. 681835-FLUDYCO-ERC-2015-CoG.

References

- [1] B. R. Sutherland, *Internal Gravity Waves*, Cambridge University Press, Cambridge, UK, 2010.
- [2] C. Aerts, J. Christensen-Dalsgaard, D. W. Kurtz, *Asteroseismology*, Springer Science & Business Media, Netherlands, 2010.
- [3] T. Rogers, D. N. Lin, H. H. B. Lau, “Internal gravity waves modulate the apparent misalignment of exoplanets around hot stars”, *Astrophys. J. Lett.* **758** (2012), no. 1, p. L6.
- [4] M. Baldwin, L. Gray, T. Dunkerton, K. Hamilton, P. Haynes, W. Randel, J. Holton, M. Alexander, I. Hirota, T. Horinouchi *et al.*, “The quasi-biennial oscillation”, *Rev. Geophys.* **39** (2001), no. 2, p. 179-229.
- [5] C. B. Leovy, A. J. Friedson, G. S. Orton, “The quasiquadrennial oscillation of Jupiter’s equatorial stratosphere”, *Nature* **354** (1991), no. 6352, p. 380.
- [6] T. Fouchet, S. Guerlet, D. Strobel, A. Simon-Miller, B. Bézard, F. Flasar, “An equatorial oscillation in Saturn’s middle atmosphere”, *Nature* **453** (2008), no. 7192, p. 200.
- [7] R. S. Lindzen, J. R. Holton, “A theory of the quasi-biennial oscillation”, *J. Atmos. Sci.* **25** (1968), no. 6, p. 1095-1107.
- [8] J. R. Holton, R. S. Lindzen, “An updated theory for the quasi-biennial cycle of the tropical stratosphere”, *J. Atmos. Sci.* **29** (1972), no. 6, p. 1076-1080.
- [9] R. Plumb, “The interaction of two internal waves with the mean flow: Implications for the theory of the quasi-biennial oscillation”, *J. Atmos. Sci.* **34** (1977), no. 12, p. 1847-1858.
- [10] A. Renaud, L.-P. Nadeau, A. Venaille, “Periodicity disruption of a model quasibiennial oscillation of equatorial winds”, *Phys. Rev. Lett.* **122** (2019), no. 21, article ID 214504.
- [11] R. Plumb, A. McEwan, “The instability of a forced standing wave in a viscous stratified fluid: A laboratory analogue of the quasi-biennial oscillation”, *J. Atmos. Sci.* **35** (1978), no. 10, p. 1827-1839.
- [12] B. Semin, N. Garroum, F. Pétrélis, S. Fauve, “Nonlinear saturation of the large scale flow in a laboratory model of the quasibiennial oscillation”, *Phys. Rev. Lett.* **121** (2018), no. 13, article ID 134502.
- [13] F. Lott, L. Guez, “A stochastic parameterization of the gravity waves due to convection and its impact on the equatorial stratosphere”, *J. Geophys. Res.* **118** (2013), no. 16, p. 8897-8909.
- [14] N. Butchart, J. Anstey, K. Hamilton, S. Osprey, C. McLandress, A. Bushell, Y. Kawatani, Y.-H. Kim, F. Lott, J. Scinocca *et al.*, “Overview of experiment design and comparison of models participating in phase 1 of the SPARC Quasi-Biennial Oscillation initiative (QBOi)”, *Geosci. Model Dev.* **11** (2018), no. 3, p. 1009-1032.
- [15] A. Bushell, J. Anstey, N. Butchart, Y. Kawatani, S. Osprey, J. Richter, F. Serva, P. Braesicke, C. Cagnazzo, C.-C. Chen *et al.*, “Evaluation of the Quasi-Biennial Oscillation in global climate models for the SPARC QBO-initiative”, *Q. J. R. Meteorol. Soc.* (2020), p. 1-31.
- [16] M. Le Bars, D. Lecoanet, S. Perrard, A. Ribeiro, L. Rodet, J. M. Aurnou, P. Le Gal, “Experimental study of internal wave generation by convection in water”, *Fluid Dyn. Res.* **47** (2015), no. 4, article ID 045502.
- [17] D. Lecoanet, M. Le Bars, K. J. Burns, G. M. Vasil, B. P. Brown, E. Quataert, J. S. Oishi, “Numerical simulations of internal wave generation by convection in water”, *Phys. Rev. E* **91** (2015), no. 6, article ID 063016.
- [18] L.-A. Couston, D. Lecoanet, B. Favier, M. Le Bars, “Dynamics of mixed convective–stably-stratified fluids”, *Phys. Rev. Fluids* **2** (2017), no. 9, article ID 094804.
- [19] L.-A. Couston, D. Lecoanet, B. Favier, M. Le Bars, “Order out of chaos: slowly reversing mean flows emerge from turbulently generated internal waves”, *Phys. Rev. Lett.* **120** (2018), no. 24, article ID 244505.
- [20] L.-A. Couston, D. Lecoanet, B. Favier, M. Le Bars, “The energy flux spectrum of internal waves generated by turbulent convection”, *J. Fluid Mech.* **854** (2018), article ID R3.
- [21] P. Léard, B. Favier, P. Le Gal, M. Le Bars, “Coupled convection and internal gravity waves excited in water around its density maximum at 4 °C”, *Phys. Rev. Fluids* **5** (2020), no. 2, article ID 024801.
- [22] J. K. Ansong, B. R. Sutherland, “Internal gravity waves generated by convective plumes”, *J. Fluid Mech.* **648** (2010), p. 405-434.
- [23] J. W. Deardorff, G. E. Willis, D. K. Lilly, “Laboratory investigation of non-steady penetrative convection”, *J. Fluid Mech.* **35** (1969), no. 1, p. 7-31.
- [24] M. Michaelian, T. Maxworthy, L. Redekopp, “The coupling between turbulent, penetrative convection and internal waves”, *Eur. J. Mech. B* **21** (2002), no. 1, p. 1-28.
- [25] A. Townsend, “Natural convection in water over an ice surface”, *Q. J. R. Meteorol. Soc.* **90** (1964), no. 385, p. 248-259.
- [26] S. Perrard, M. Le Bars, P. Le Gal, “Experimental and numerical investigation of internal gravity waves excited by turbulent penetrative convection in water around its density maximum”, in *Studying Stellar Rotation and Convection*, Springer, Berlin, Heidelberg, Germany, 2013, p. 239-257.
- [27] L. N. Howard, “Convection at high Rayleigh number”, in *Applied Mechanics*, Springer, New York, USA, 1966, p. 1109-1115.
- [28] K. J. Burns, G. M. Vasil, J. S. Oishi, D. Lecoanet, B. P. Brown, “Dedalus: A flexible framework for numerical simulations with spectral methods”, *Phys. Rev. Res.* **2** (2020), no. 2, article ID 023068.
- [29] P. Fisher, J. Lottes, S. Kerkemeier, “Nek5000 v17.0”, <http://nek5000.mcs.anl.gov> (2017).

- [30] D. Lecoanet, M. Cantiello, E. Quataert, L.-A. Couston, K. J. Burns, B. J. Pope, A. S. Jermyn, B. Favier, M. Le Bars, “Low-frequency variability in massive stars: Core generation or surface phenomenon?”, *Astrophys. J. Lett.* **886** (2019), no. 1, p. L15.
- [31] M. J. Lighthill, *Waves in Fluids*, Cambridge University Press, Cambridge, UK, 2001.
- [32] P. Goldreich, P. Kumar, “Wave generation by turbulent convection”, *Astrophys. J.* **363** (1990), no. 2, p. 694-704.
- [33] D. Lecoanet, E. Quataert, “Internal gravity wave excitation by turbulent convection”, *Mon. Not. R. Astron. Soc.* **430** (2013), no. 3, p. 2363-2376.
- [34] D. M. Bowman, S. Bursens, M. G. Pedersen, C. Johnston, C. Aerts, B. Buysschaert, M. Michielsen, A. Tkachenko, T. M. Rogers, P. V. Edelman *et al.*, “Low-frequency gravity waves in blue supergiants revealed by high-precision space photometry”, *Nat. Astron.* **3** (2019), no. 8, p. 760-765.
- [35] P. Edelman, R. Ratnasingham, M. Pedersen, D. Bowman, V. Prat, T. Rogers, “Three-dimensional simulations of massive stars. I. Wave generation and propagation”, *Astrophys. J.* **876** (2019), no. 1, p. 4.
- [36] D. Bowman, “What physics is missing in theoretical models of high-mass stars: new insights from asteroseismology”, *preprint*, arXiv:1912.12653 (2019).
- [37] T. Crueger, M. A. Giorgetta, R. Brokopf, M. Esch, S. Fiedler, C. Hohenegger, L. Kornblueh, T. Mauritsen, C. Nam, A. K. Naumann *et al.*, “ICON-A, the atmosphere component of the ICON earth system model: II. Model evaluation”, *J. Adv. Model. Earth Syst.* **10** (2018), no. 7, p. 1638-1662.
- [38] J. A. Anstey, J. F. Scinocca, M. Keller, “Simulating the QBO in an atmospheric general circulation model: Sensitivity to resolved and parameterized forcing”, *J. Atmos. Sci.* **73** (2016), no. 4, p. 1649-1665.
- [39] L.-A. Couston, D. Lecoanet, B. Favier, M. Le Bars, “Shape and size of large-scale vortices: A generic fluid pattern in geophysical fluid dynamics”, *Phys. Rev. Res.* **2** (2020), no. 2, article ID 023143.
- [40] S. Labrosse, “Thermal evolution of the core with a high thermal conductivity”, *Phys. Earth Planet. Inter.* **247** (2015), p. 36-55.
- [41] E. Jaupart, B. Buffett, “Generation of MAC waves by convection in Earth’s core”, *Geophys. J. Int.* **209** (2017), no. 2, p. 1326-1336.